Anti-hypertrophic effect of Na+/H+ exchanger-1 inhibition is mediated by reduced cathepsin B

Sadaf Riaz, Nabeel Abdulrahman, Shahab Uddin, Ayesha Jabeen, Alain P. Gadeau, Larry Fliegel, Fatima Mraiche

Anti-hypertrophic effect of Na^+/H^+ exchanger-1 inhibition is mediated by reduced cathepsin B

Sadaf Riaz, Nabeel Abdulrahman, Shahab Uddin, Ayesha Jabeen, Alain P. Gadeau, Larry Fliegel, Fatima Mraiche

PII: S0014-2999(20)30512-4

DOI: https://doi.org/10.1016/j.ejphar.2020.173420

Reference: EJP 173420

To appear in: *European Journal of Pharmacology*

Received Date: 23 June 2020

Revised Date: 24 July 2020

Accepted Date: 24 July 2020

Please cite this article as: Riaz, S., Abdulrahman, N., Uddin, S., Jabeen, A., Gadeau, A.P, Fliegel, L., Mraiche, F., Anti-hypertrophic effect of Na^+/H^+ exchanger-1 inhibition is mediated by reduced cathepsin B, *European Journal of Pharmacology*, https://doi.org/10.1016/j.ejphar.2020.173420.

Mraiche F: Conceptualization, Methodology, Formal analysis, Validation, Writing-Original Draft, Writing-Reviewing & Editing, Visualization, Supervision, Project Administration, Funding Acquisition, Resources. **Riaz S:** Conceptualization, Methodology, Formal analysis, Validation, Investigation, Writing-Original Draft, Writing-Review & Editing, Visualization. **Abdulrahman N:** Formal analysis, Validation, Investigation, Writing-Review & Editing. **Jabeen A:** Formal analysis, Investigation. **Gadeau AP:** Investigation, Formal analysis, Writing - Review & Editing. **Uddin S:** Formal analysis, Writing-Review & Editing, Resources. **Fliegel L:** Formal analysis, Writing - Review & Editing.

Anti-hypertrophic effect of Na^+/H^+ exchanger-1 inhibition is mediated by reduced cathepsin B.

Sadaf Riaz[a,b], Nabeel Abdulrahman[a,c], Shahab Uddin[c], Ayesha Jabeen[a], Alain P Gadeau[d], Larry Fliegel[e], Fatima Mraiche[a*]

[a]College of Pharmacy, QU Health, Qatar University, Doha, Qatar

[b]Hamad Medical Corporation, Doha, Qatar

[c]Translational Research Institute, Academic Health System, Hamad Medical Corporation, Doha, Qatar

[d]University of Bordeaux, UMR1034, Pessac, France

[e]University of Alberta, Edmonton, Alberta, Canada

*__Corresponding author:__ Dr. Fatima Mraiche, College of Pharmacy, QU Health, Qatar University, P.O. Box 2713, Doha, Qatar. Telephone: +974 4403 5594; Fax: +974 4403 5551; E-mail: fatima.mraiche@qu.edu.qa.

Abstract

Previous studies have established the role of Na^+/H^+ exchanger isoform-1 (NHE1) and cathepsin B (Cat B) in the development of cardiomyocyte hypertrophy (CH). Both NHE1 and Cat B are activated under acidic conditions suggesting that their activities might be interrelated. The inhibition of NHE1 has been demonstrated to reduce cardiac hypertrophy but the mechanism that contributes to the anti-hypertrophic effect of NHE1 inhibition still remains unclear. H9c2 cardiomyoblasts were stimulated with Angiotensin (Ang) II in the presence and absence of N-[2-methyl-4,5-bis(methylsulphonyl)-benzoyl]-guanidine, hydrochloride (EMD, EMD 87580), an NHE1 inhibitor or CA-074Me, a Cat B inhibitor, and various cardiac hypertrophic parameters, namely cell surface area, protein content and atrial natriuretic peptide (ANP) mRNA were analyzed. EMD significantly suppressed markers of cardiomyocyte hypertrophy and inhibited Ang II stimulated Cat B protein and gene expression. Cat B is located within the acidic environment of lysosomes. Cat B proteases are released into the cytoplasm upon disintegration of the lysosomes. EMD or CA-074Me prevented the dispersal of the lysosomes induced by Ang II and reduced the ratio of LC3-II to LC3-I, a marker of autophagy. Moreover, Cat B protein expression and MMP-9 activity in the extracellular space were significantly attenuated in the presence of EMD or CA-074Me. Our study demonstrates a novel mechanism for attenuation of the hypertrophic phenotype by NHE1 inhibition that is mediated by a regression in Cat B. The inhibition of Cat B via EMD or CA-074Me attenuates the autosomal-lysosomal pathway and MMP-9 activation.

Key words: cardiomyocytes, hypertrophy, autophagy, cathepsins, angiotensin, matrix metalloproteinases.

1. Introduction

Cardiovascular diseases (CVDs) continue to be the major reason for death globally, regardless of the progress in treatment (WHO, 2013). The World Health Organization forecasts that by 2030, heart failure will be a leading cause of death (Mathers CD, 2006; WHO, 2011). Various CVDs including cardiac hypertrophy (CH), hypertension and myocardial infarctions progress to heart failure if left untreated (de Couto et al., 2010; Dupree, 2010). Pathological CH, induced by neurohormonal stimulation, hypertension or myocardial infarctions (MI), is characterized by the increase in size of cardiomyocytes and the remodeling of the extracellular matrix (ECM) (Kang and Izumo, 2003; Kehat and Molkentin, 2010; Mlih et al., 2015; Watkins et al., 2011). The abnormal stimulation of various ECM proteases including cathepsins and matrix metalloproteinases (MMPs) have been proposed to contribute to the progression of cardiac remodeling (Abdulrahman et al., 2018; Cheng et al., 2012; Dhalla et al., 2009; Rodriguez et al., 2010; Wilson EM, 2001).

The cysteine proteases, cathepsins, have been demonstrated to contribute to cardiac remodeling (Brömme and Wilson, 2011; Liu et al., 2013; Müller and Dhalla, 2012; Wu et al., 2015). Previous studies have demonstrated that stimulation of H9c2 cardiomyoblasts with Ang II, a hypertrophic stimulator (Wu et al., 2015). Cat B protein expression and the inhibition of Cat B resulted in attenuation of cardiomyocyte hypertrophy (Wu et al., 2015). Similarly, *in vivo,* the knockout of Cat B attenuated pressure overload-induced CH, fibrosis, and apoptosis (Wu et al., 2015). Cat B mRNA and protein expression were demonstrated to be increased in human dilated cardiomyopathy (Ge et al., 2006). Clearly, Cat B has a crucial function in hypertrophy.

Acidification of the peri- and extracellular spaces in settings of altered cell proliferation has been shown to activate Cat B (Bourguignon et al., 2004; Greco et al., 2014; Rozhin et al., 1994). In various forms of carcinomas, this type of pericellular acidification is caused by the stimulation of the Na^+/H^+ exchanger isoform 1 (NHE1), a regulator of intracellular pH (Bourguignon et al., 2004; Malo and Fliegel, 2006). NHE1 is a ubiquitously expressed housekeeping glycoprotein, which exchanges one intracellular H^+ for one extracellular Na^+ and is the only cardiac specific plasma membrane isoform of the NHE family (Mohamed and Mraiche, 2015). Increased activation of NHE1 is a key factor for the development of various CVDs including CH (Fliegel, 2009; Liu et al., 2013; Wu et al., 2015; Xue et al., 2010). Inhibition of NHE1, both *in vivo* and *in vitro,* has been demonstrated to regress hypertrophy (Javadov et al., 2008; Javadov et al., 2009; Marano et al., 2004; Mohamed and Mraiche, 2015). The cellular mechanism by which NHE1 inhibition suppresses the hypertrophic response is not known. However, stimulation of NHE1 is known to promote Cat B activity in breast cancer cells (Bourguignon et al., 2004) suggesting that NHE1 and Cat B activities might be related. Whether the anti-hypertrophic effects of NHE1 inhibitors act downstream through Cat B in cardiomyocytes is not known.

It has also been suggested that in a malignant cell line, an increase in the pericellular acidic pH results in the relocation of the lysosomes. The acidic pericellular pH also enhances the secretion of Cat B into the extracellular space (Rozhin et al., 1994). Furthermore, the release of Cat B into the ECM induces the activation of MMP-9 (Giusti et al., 2008). In the myocardium, MMP-9 contributes to ECM remodeling and failure (Singh et al., 2004; Stempien-Otero et al., 2006). Interestingly, MMP-9 activity has also been demonstrated to be enhanced in CCL39 lung fibroblasts upon the activation of NHE1 with phenylephrine (Taves et al., 2008). Recently, the interaction of Cat B and MMP-9 with NHE1 has been shown to

promote ECM degradation in breast cancer (Greco et al., 2014). These studies suggest a putative pathway by which NHE1 inhibition reduces Cat B and in turn prevents MMP-9 activation and protects against hypertrophy.

To verify the role of Cat B in the anti-hypertrophic effect of NHE1 inhibition, we examined the effect of the NHE1-specific inhibitor *N*-[2-methyl-4,5-bis(methylsulphonyl)-benzoyl]-guanidine, hydrochloride (EMD, EMD87580; 10 μM) on the hypertrophic phenotype, Cat B protein and mRNA expression, Microtubule‑associated protein light chain 3 (LC3)-I/II protein expression and MMP-9 activity in Ang II-treated H9c2 cardiomyoblasts.

2. Materials and methods

2.1.Materials

All routine chemicals were obtained from BD Biosciences (San Jose, CA), Fisher Scientific (Ottawa, ON) or Sigma (St. Louis, MO). EMD 87580 (EMD) was a generous gift from Dr. N. Beier of Merck KGaA (Frankfurt, Germany). Primary antibodies used for Western blotting including rabbit polyclonal Cat B (sc-13985) (Amantini et al., 2015) and rabbit polyclonal MMP-9 (sc-10737)(Li et al., 2014) were purchased from Santa Cruz Biotechnology (Santa Cruz, CA). Rabbit polyclonal anti-NHE1 (ab67314) and α-tubulin (ab4074) antibodies were from Abcam (Cambridge, MA). Rabbit polyclonal anti-LC3 A/B (12741) was from Cell Signaling. Secondary antibodies were purchased from Abcam.

2.2.Cell culture

H9c2 myoblasts, a clonal cell line derived from the embryonic BD1X rat heart tissue (Hescheler et al., 1991) were obtained from European Collections of Cell Cultures (ECACC)

and cultured in DMEM/F12 1:1 culture media supplemented with 10% fetal bovine serum (FBS) and 1% penicillin/streptomycin at 37°C in a humidified atmosphere (95% O_2-5% CO_2) (Hescheler et al., 1991; Riaz, 2016). Watkins et al. 2011 has recently demonstrated that the H9c2 cell line shows a similar hypertrophic response to primary neonatal cardiomyocytes including membrane morphology, G-signaling protein expression and electrophysiological properties (Watkins et al., 2011). In addition, Watkins et al (Watkins et al., 2011) and others have demonstrated that the H9c2 cell line had hypertrophy-associated traits when stimulated with hypertrophic agents *in vitro*. Cardiomyoblasts were seeded at a density of 2 x 10^5 cells in 35 mm culture dishes. The cells were starved in serum free maintenance media for 24 h, and treated with Ang II (10 µM), Ang II+EMD (EMD 87580; NHE1 inhibitor), Ang II+CA-074 Methyl Ester (Me); Cat B inhibitor), EMD (10 µM), or CA-074Me (10 µM) alone for 24 h. Ang II and EMD were dissolved in distilled water and CA-074Me was dissolved in dimethyl sulfoxide (DMSO).

2.3.Western blot analysis

H9c2 cardiomyoblasts were lysed using radio-immunoprecipitation protein assay (RIPA) buffer as described earlier (Mraiche and Fliegel, 2011) (Fliegel, 2009; Liu et al., 2013; Wu et al., 2015; Xue et al., 2010). Briefly, cell lysates were centrifuged at 16,000 g for 15 min at 4°C and the supernatant containing the proteins were collected (Riaz, 2016). Total amount of protein present was quantified using the DC protein assay kit (Biorad). 15-25 µg of protein was separated on 15% or 9% SDS-PAGE and transferred on to nitrocellulose membranes. The membranes were probed with anti-Cat B antibody, which recognizes bands at 37 kDa (pro-Cat B) and 25 kDa (active-Cat B) (Bien et al., 2004), rabbit polyclonal anti-MMP-9, rabbit polyclonal anti-NHE1, rabbit polyclonal anti-LC3 A/B. Anti-α-tubulin was used as a loading control. Immunoreactive proteins were visualized using enhanced

chemiluminescence (Amersham Biosciences) and imaged using the Alpha Innotech FluorChem Imager (R&D Systems). The images of the western blot bands were then quantified using Scion Image software (Scion Corporation) by densitometry analysis (Sotanaphun et al., 2009).

2.4.Gelatin Zymography

Non reduced protein samples (80 µg) were loaded on to resolving gels prepared by including 0.2% final concentration gelatin to acrylamide polymerization mixture (Riaz, 2016). After SDS PAGE, the gels were washed with 2.5 % Triton X-100 and then incubated for 24 h at 37°C in substrate buffer (50 mM Tris HCl, 0.15 M NaCl, 5 mM $CaCl_2$, and 0.05% NaN_3, pH 7.6). The gels were stained with 1% Coomassie blue R-250 in acetic acid:methanol:water (1:2.5:6.5) for 1 h and then destained with the same solvent. The gels were then imaged to observe gelatinolytic activity.

2.5.Reverse Transcription-Polymerase Chain Reaction (RT-PCR)

RNA was extracted from cultured cells using TRIzol reagent and the concentration of RNA was determined using spectrophotometer (Nanodrop 2000c, Thermo Scientific). cDNA was synthesized by reverse transcribing 2 µg of total RNA using High capacity cDNA Reverse Transcription Kit (Applied Biosystems) (Riaz, 2016). The cDNA product was amplified using thermal cycler (Mastercycler, Eppendorf). 50-175 ng from the cDNA product was used for each PCR reaction. The PCR steps included initial denaturation of samples for 3 min at 94°C followed by 35 cycles of denaturation (94°C for 45 s), annealing (60°C for 30 s) and extension (72°C for 1 min). The reaction ended with a final extension (72°C for 10 min). Cat B cDNA was amplified using 5′-GGGGGAAATCTACAAAAATG-3′ and antisense 5′-AAAGACTCCTATCTGCCTCACT-3′ and ANP cDNA was amplified using sense 5′-

CTGCTAGACCACCTGGAGGA-3, antisense 5′-AAGCTGTTGCAGCCTAGTCC-3. The control β-actin cDNA was primed with sense 5′-GTTCCGATGCCCGAGGCTCT-3′ and antisense 5′-GCATTTGCGTGCACAGATGGA-3′. PCR products were then electrophoresed on 2% agarose gels stained with ethidium bromide. Cat B and ANP mRNA bands were imaged using the Alpha Innotech FluorChem Imager. The changes in Cat B and ANP mRNA levels were normalized to β-actin and quantified using Scion Image software.

2.6.Measurement of cell surface area of H9c2 cardiomyoblasts

Briefly, cardiomyoblasts were seeded in 35 mm culture dishes at a density of 3 x 10^4 cells per dish (Riaz, 2016). After treatment period, the cells were rinsed with 1X Phosphate Buffer Saline (PBS), fixed with 4% formaldehyde and stained with 0.5% crystal violet in 2% ethanol. A minimum of 10 representative cells were considered from three dishes, the average of which represented as one n value. Cell surface area was calculated using AxioVision Imaging software (Carl Zeiss Microimaging).

2.7.Measurement of protein content of H9c2 cardiomyoblasts

Protein content was measured as described previously (Merten et al., 2006). Briefly, control and treated cardiomyoblasts were harvested with trypsin (Riaz, 2016). The total number of cardiomyoblasts present per dish is counted with a hemocytometer. Protein concentration of cardiomyoblasts lysed with RIPA buffer was determined with Biorad DC protein assay kit. Protein content was calculated by dividing total amount of protein (μg) by the total number of cardiomyoblasts.

2.8.Localization of the lysosomes

Briefly, following treatment, cardiomyoblasts were incubated with a cell permeable

acidotropic probe, namely, LysoTracker Red DND-99 (75 µM) (Invitrogen) for 30 min, which selectively binds to vacuoles with low internal pH (Riaz, 2016). The cells were then incubated with 1 µM HOECST for another 30 min. Finally, the cells were viewed under a fluorescence microscope (OlympusIX70; Olympus Corp).

2.9.Statistical Analysis

Values were expressed as % control ± S.E.M. Student t test and ANOVA followed by Bonferroni was used to calculate differences between groups where a $P<0.05$ was considered significant.

3. Results

3.1.Ang II stimulates a concentration dependent increase in Cat B protein expression in H9c2 cardiomyoblasts

H9c2 cardiomyoblasts were treated with 1, 10, or 100 µM, or 1, 10, or 100 nM Ang II for 24. Western blot analysis showed that stimulation with 10 uM Ang II significantly increased ($P<0.05$) (Fig. 1A and B) the expression of pro-Cat B (37 kDa) and active-Cat B (25 kDa) protein (Bien et al., 2004). A concentration of 100 µM Ang II induced significant cell death which was confirmed by counting the number of cardiomyoblasts using a hemocytometer and comparing it to the non-treated set. This could likely be the reason for a decrease in Cat B protein expression at 100 µM.

3.2.Effect of EMD or CA-074Me on hypertrophy

Previous reports have demonstrated that induction of cardiomyocyte hypertrophy due to various extracellular stimuli could be reduced by NHE1 inhibitors (Javadov et al., 2009;

Marano et al., 2004; Mohamed and Mraiche, 2015). In our study, 10 μM of Ang II significantly enhanced the expression of ANP mRNA ($P< 0.05$) (Fig. 2A and B), total protein content ($P< 0.05$) (Fig. 2C) and cell surface area ($P< 0.05$) (Fig. 2D and E) in H9c2 cardiomyoblasts. These effects were significantly regressed in the presence of EMD or CA-074Me.

3.3.Effect of EMD on Cat B protein and gene expression

Protein and RNA samples extracted from EMD treated H9c2 cardiomyoblasts were subjected to Western blotting and RT PCR, respectively, to identify whether Cat B protein and mRNA expression are interrelated to the anti-hypertrophic property of EMD. Immunoblot and gene amplification analysis showed that Cat B protein and gene expression were significantly enhanced following treatment with 10 μM Ang II ($P<0.05$), an effect that was significantly reduced in the presence of EMD ($P<0.05$) (Fig. 3A-D). Similarly, Cat B protein and gene expression were significantly reduced when pre-treated with CA-074Me ($P<0.05$) (Fig. 3A-D).

3.4.Effect of EMD or CA-074Me on lysosomal integrity

The acidic environment within the lysosomes facilitates the localization of Cat B and functions to degrade and eliminate unwanted proteins (Cheng et al., 2012). In order to identify the effect of EMD or CA-074Me on the localization and morphology of lysosomes, H9c2 cardiomyoblasts treated with 10 μM Ang II in the presence of EMD or CA-074Me were stained with acidotropic probe LysoTracker Red. Stimulation of cardiomyoblasts with Ang II revealed an increased distribution and dispersion of the lysosomes when compared to the non-treated (Fig. 4A). Treatment with EMD or CA-074Me prevented the distribution of the lysosomes induced by Ang II (Fig. 4A).

3.5.Effect of EMD on Cat B protein expression in the extracellular environment

Our findings suggest that treatment with EMD results in less dispersion and distribution of the lysosomes, which may be indicative of less extrusion of Cat B into the extracellular media. Hence, we assessed the levels of Cat B in conditioned media of H9c2 cardiomyoblasts treated with Ang II in the presence or absence of EMD or CA-074Me. Western blot analysis showed that Ang II treatment significantly increased Cat B protein (P<0.05) (Fig. 4B and C). The increase Cat B protein expression was significantly reduced in the presence of EMD (P<0.05) (Fig. 4B and C). Similarly, pre-treatment with CA-074Me significantly reduced the Cat B protein expression in the media (P<0.05) (Fig. 4B and C).

3.6.Effect of EMD on MMP-9 gelatinolytic activity

A recent study has shown that acidification of the extracellular space increases the secretion of MMP-9 and Cat B (Greco et al., 2014). It was also identified that Cat B is involved in the pH dependent activation of pro-MMP-9 (Giusti et al., 2008). Hence, we examined MMP-9 activity in the conditioned media of H9c2 cardiomyoblasts stimulated with Ang II in the presence or absence of EMD or CA-074Me treatment. Gelatin zymography showed that MMP-9 gelatinolytic activity was significantly increased following stimulation with 10 µM Ang II (P<0.05) (Fig. 4D and E), an effect that was significantly reduced upon stimulation with EMD (P<0.05) (Fig. 4D and E). Similarly, pre-treatment with CA-074Me significantly lowered MMP-9 activity (P<0.05) (Fig. 4D and E).

3.7.Effect of EMD on the autophagic response

Stress activated autophagy-lysosomal pathway is regulated by Cat B (activated by acidic pH) and NHE1 (Sun et al., 2013). LC3 II/I protein expression is generally used to assess

autophagy. The level of LC3-II and LC3-I proteins were measured by immunoblot analysis in H9c2 cardiomyoblasts treated with 10 µM Ang II in the presence and absence of EMD or CA-074Me. Our results revealed that the ratio of LC3-II to LC3-I protein expression was significantly elevated following treatment with 10 µM Ang II ($P<0.05$) (Fig. 5A and B). This effect was significantly reduced upon treatment with EMD ($P<0.05$) or CA-074Me ($P<0.05$) (Fig. 5A and B).

4. Discussion

Activation and enhanced expression of NHE1 and proteases such as cathepsins have been proposed to contribute to CH (Cheng et al., 2012; Müller and Dhalla, 2012). NHE1 inhibitors have been shown to regress the hypertrophic response to various extracellular stimuli (Giusti et al., 2008; Kostoulas et al., 1999). Interestingly, Cat B in a breast cancer model was shown to be activated in response to a fall in the extracellular pH mediated by over active NHE1 (Bourguignon et al., 2004). In addition, Cat B was demonstrated to directly interrelate with NHE1 and cause ECM degradation (Greco et al., 2014). Whether the anti-hypertrophic effect of NHE1 inhibition occurs due to the attenuation of Cat B remains unclear.

4.1.Ang II induces the expression of Cat B in H9c2 cardiomyoblasts

The role of Cat B in cardiac remodeling has been demonstrated in *in vitro, in vivo* and in human failing hearts. A previous *in vitro* study demonstrated that inhibition of Cat B reduced cardiac hypertrophy mediated through ASK1/JNK pathway (Wu et al., 2015). *In vivo,* pressure overload induced cardiac remodeling process was attenuated in the absence of Cat B (Wu et al., 2015). Moreover, the inhibition of Cat B with CA-074Me resulted in significant reduction of cardiomyocyte size, cardiac fibrosis and attenuated cardiac dysfunction. (Liu et

al., 2013). The expression of Cat B mRNA and protein were significantly higher in failing hearts compared with non-failing hearts (Ge et al., 2006).

Our findings are in accordance with a previous study, which has demonstrated that Ang II induces Cat B expression/activity in the current study, both the pro and active-Cat B protein were significantly elevated in H9c2 cardiomyoblasts when treated with 10 μM Ang II (Fig. 1A and B). Similarly, Wu *et al* showed that Ang II increased Cat B protein expression in H9c2 cardiomyoblasts (Wu et al., 2015).

Other cathepsin isoforms have also been implicated in cardiac remodeling and hypertrophy (Müller and Dhalla, 2012). A previous study showed that gene and protein levels of Cat S, B, and L were increased in cultured neonatal rat cardiomyocytes (Cheng et al., 2006). Similarly, Cat S has been shown to be elevated in the myocardium of rats linked with hypertension induced heart failure (Cheng et al., 2006). Cat S were also enhanced in hearts obtained from humans with heart failure (Cheng et al., 2006). Phenylephrine-induced CH was more prominent in the absence of Cat L, *in vitro* (Sun et al., 2013). Another study reported that MI induced by left coronary artery ligation in wild-type rats caused rapid Cat L activation in the myocardium and its deficiency resulted in reduced cardiac function and survival post-MI (Sun et al., 2011). Moreover, Cat S deficiency enhanced cardiac fibrosis stimulated by Ang II (Pan et al., 2012). Although many forms of cathepsins have been proposed to contribute to CH, in our study we focused on Cat B, which is stimulated by an acidic pH (Bourguignon et al., 2004; Rozhin et al., 1994), a major stimulus of NHE1 activity. Whether the various forms of cathepsins are simultaneously upregulated in a model of hypertrophy or the interplay between the various forms of cathepsins remains unknown.

4.2.EMD reduces Cat B mediated hypertrophy

In order to identify the role of Cat B in promoting hypertrophy, three hypertrophic markers namely, ANP mRNA, protein content and cell area were analyzed. Our results showed that 10 µM Ang II induced hypertrophy in H9c2 cardiomyoblasts (Fig. 2A-E). Inhibition of NHE1 or Cat B significantly decreased the hypertrophic effect (Fig. 2A-E). Pre-treatment with EMD significantly reduced Cat B protein and gene expression (Fig. 3A-D). Our results demonstrate for the first time that EMD reduced Cat B protein and mRNA expression in H9c2 cardiomyoblasts. Our findings reveal for the first time that the anti-hypertrophic effect of NHE1 inhibition may occur in part by reduced Cat B expression (Riaz, 2016).

4.3.EMD or CA-074 reduces Cat B protein expression through MMP-9 activity

The acidic environment within the lysosomes facilitates localization of Cat B where it becomes functional to degrade and eliminate defective proteins (Cheng et al., 2012). A previous report has confirmed that relocation of lysosomes to cell edge and secretion of Cat B is associated with an acidic extracellular pH. Interestingly, this effect was inhibited with various broad and specific NHE inhibitors (Steffan et al., 2009). Hence, we focused to analyze the intracellular localization of lysosomes using the acidotropic probe LysoTracker Red in H9c2 cardiomyoblasts stimulated with Ang II in the presence and absence of EMD. Treatment with EMD or CA-074Me resulted in less distribution and dispersion of the lysosomes (Fig. 4A), which may be indicative of less secretion of Cat B into the extracellular media. The dispersion of the lysosomes can result in the release of the Cat B proteases into the cytosol or into the extracellular compartment (Rozhin et al., 1994). Our study demonstrated for the first time that pro-Cat B protein levels were significantly increased in the extracellular compartment (Fig. 4B and C), an effect that was significantly reduced EMD or CA-074Me (Fig. 4B and C). It is to be noted that the pro-Cat B is enzymatically inactive,

however studies have shown that pro-Cat B can also be induced by interactions with matrices, for example, human prostate carcinoma cells with collagen I gels or human bone explants (Mundel and Reiser, 2010). It has been demonstrated that pro-Cat L could be activated by heparan sulphate (Ishidoh and Kominami, 1995).

A previous study demonstrated that pro-Cat B retains some of its catalytic activity and as such, is capable of activating pro-MMP-9 (Giusti et al., 2008; Pungercar et al., 2009). Moreover, an *in vivo* study showed that CH does not occur in MMP-9 deficient mice after Ang II treatment, which suggests that MMP-9 has a crucial role in Ang II-induced cardiac hypertrophy (Weng et al., 2016). Therefore, we analyzed the MMP-9 gelatinolytic activity in the conditioned media. Gelatin zymography revealed that MMP-9 gelatinolytic activity was significantly increased in conditioned media from H9c2 cardiomyoblasts treated with Ang II (Fig. 4D and E). However, this effect was significantly reduced upon the inhibition of NHE1 or Cat B (Fig. 4D and E). In our study, MMP-9 was detected only at 92 kDa in the gelatin zymograms, which is in agreement with previous studies (Giusti et al., 2008; Solli et al., 2013). The band corresponding to 92 kDa is mostly described as the inactive MMP-9. However, certain protein substrates have been shown to cause conformational changes within the MMP-9 structure that result in the exposure of the active site without cleavage of the pro-peptides (Fedarko et al., 2004; Freise et al., 2009).

4.4.EMD maintains the autosomal-lysosomal pathway

Deregulation of various signaling pathways and cardiomyocyte autophagy lead to the development of pathological CH (Frey and Olson, 2003; Heineke and Molkentin, 2006). Foregoing research also proved that regulation of pH by NHE1 is crucial in regulating autophagy in order to eliminate defective proteins (Togashi et al., 2013). Whether the anti-

hypertrophic effects of NHE1 inhibitors reduce Cat B in association with cardiomyocyte autophagy remains unclear.

LC3 is a ubiquitously found soluble protein in mammalian tissues and cultured cells (Tanida et al., 2008). During autophagy, autophagosomes engulf cytoplasmic components, including cytosolic proteins and organelles. Alongside, a cytosolic form of LC3 (LC3-I) is conjugated to phosphatidylethanolamine to form LC3-II, which is transported to autophagosome membranes (Tanida et al., 2008). The final step of the autophagy–lysosomal pathway is the fusion of an autophagosome with a functioning lysosome. LC3-II stays on the membrane until it is degraded by the lysosome. Hence, the amount of LC3‐II/LC3-I reflects autophagic activity, and detecting LC3 by immunoblotting has become a reliable and widely used marker for autophagic process (Levine and Kroemer, 2008; Mizushima and Yoshimori, 2007). It is to be noted that an imbalance of protein homeostasis by dysfunction of the autophagy-lyosomal pathway may lead to pathological hypertrophy (Sandri, 2013; Zhao et al., 2007).

Our results showed that the ratio of LC3-II/LC3-I protein expression was significantly increased (Fig. 5A and B). This effect was significantly reduced upon treatment with EMD or CA-074Me (Fig. 5A and B). Our results showed that EMD or CA-074Me in H9c2 cardiomyoblasts stimulated with Ang II reduced the expression of the ratio of LC3-II/LC3-I, which is indicative of impaired autophagy.

5. Conclusion

The inhibition of NHE1 or Cat B reduced the hypertrophic response indicating an important role of NHE1 and Cat B in the hypertrophic pathway. Our study demonstrated for the first time that inhibition of NHE1 with EMD reduced Cat B protein and gene expression

suggesting that the anti-hypertrophic effect of EMD, an NHE1 inhibitor, is mediated by Cat B. Furthermore, inhibition of NHE1 and Cat B resulted in less dispersion of the lysosomes and also reduced the protein expression of the LC3II to LC3-I ratio. This suggests that the autophagy-lysosomal pathway plays a role in mediating the anti-hypertrophic. Dispersion of the lysosomes resulted in the secretion of Cat B into the extracellular space where it activated pro-MMP-9. These effects were reduced upon inhibition of NHE1 or Cat B (Fig 6) (Riaz, 2016). The extent to which the conclusions of the present work may be applicable to native cardiomyoblasts and *in vivo* heart will require further studies using appropriate animal models. This shall confirm the results obtained in the present study.

Funding: This publication was supported by Qatar University Internal Grant No. QUUG-CPH-CPH-15/16-9. "The funders had no role in study design, data collection and analysis, decision to publish, or preparation of the manuscript." The authors declare no conflict of interest.

Author contributions: Participated in research design: Sadaf Riaz, Fatima Mraiche

Conducted experiments: Sadaf Riaz, Nabeel Abdulrahman, Ayesha Jabeen, Alain P Gadeau

Contributed new reagents or analytic tools: Fatima Mraiche, Shahab Uddin

Performed data analysis: Sadaf Riaz, Nabeel Abdulrahman, Ayesha Jabeen, Fatima Mraiche

Wrote or contributed to the writing of the manuscript: Sadaf Riaz, Nabeel Abdulrahman, Alain P Gadeau, Larry Fliegel, Fatima Mraiche

Acknowledgements: The authors would like to thank Ms. Jensa Joseph for her technical support.

Ethical standards: The manuscript does not contain clinical studies or patient data.

Declaration of interest: The authors declare that they have no conflict of interest.

References

Abdulrahman, N., Jaspard-Vinassa, B., Fliegel, L., Jabeen, A., Riaz, S., Gadeau, A.P., Mraiche, F., 2018. Na(+)/H(+) exchanger isoform 1-induced osteopontin expression facilitates cardiac hypertrophy through p90 ribosomal S6 kinase. Physiological genomics 50, 332-342.

Amantini, C., Morelli, M.B., Santoni, M., Soriani, A., Cardinali, C., Farfariello, V., Eleuteri, A.M., Bonfili, L., Mozzicafreddo, M., Nabissi, M., Cascinu, S., Santoni, G., 2015. Sorafenib induces cathepsin B-mediated apoptosis of bladder cancer cells by regulating the Akt/PTEN pathway. The Akt inhibitor, perifosine, enhances the sorafenib-induced cytotoxicity against bladder cancer cells. Oncoscience 2, 395-409.

Bien, S., Ritter, C.A., Gratz, M., Sperker, B., Sonnemann, J., Beck, J.F., Kroemer, H.K., 2004. Nuclear Factor-κB Mediates Up-Regulation of Cathepsin B by Doxorubicin in Tumor Cells. Molecular Pharmacology 65, 1092-1102.

Bourguignon, L.Y., Singleton, P.A., Diedrich, F., Stern, R., Gilad, E., 2004. CD44 interaction with Na+-H+ exchanger (NHE1) creates acidic microenvironments leading to hyaluronidase-2 and cathepsin B activation and breast tumor cell invasion. The Journal of biological chemistry 279, 26991-27007.

Brömme, D., Wilson, S., 2011. Role of Cysteine Cathepsins in Extracellular Proteolysis. 23-51.

Cheng, X.W., Obata, K., Kuzuya, M., Izawa, H., Nakamura, K., Asai, E., Nagasaka, T., Saka, M., Kimata, T., Noda, A., Nagata, K., Jin, H., Shi, G.P., Iguchi, A., Murohara, T., Yokota, M., 2006. Elastolytic cathepsin induction/activation system exists in myocardium and is upregulated in hypertensive heart failure. Hypertension 48, 979-987.

Cheng, X.W., Shi, G.P., Kuzuya, M., Sasaki, T., Okumura, K., Murohara, T., 2012. Role for cysteine protease cathepsins in heart disease: focus on biology and mechanisms with clinical implication. Circulation 125, 1551-1562.

de Couto, G., Ouzounian, M., Liu, P.P., 2010. Early detection of myocardial dysfunction and heart failure. Nature reviews. Cardiology 7, 334-344.

Dhalla, N.S., Saini-Chohan, H.K., Rodriguez-Leyva, D., Elimban, V., Dent, M.R., Tappia, P.S., 2009. Subcellular remodelling may induce cardiac dysfunction in congestive heart failure. Cardiovascular research 81, 429-438.

Dupree, C.S., 2010. Primary prevention of heart failure: an update. Curr Opin Cardiol 25, 478-483.

Fedarko, N.S., Jain, A., Karadag, A., Fisher, L.W., 2004. Three small integrin binding ligand N-linked glycoproteins (SIBLINGs) bind and activate specific matrix metalloproteinases. FASEB journal : official publication of the Federation of American Societies for Experimental Biology 18, 734-736.

Fliegel, L., 2009. Regulation of the Na(+)/H(+) exchanger in the healthy and diseased myocardium. Expert Opin Ther Targets 13, 55-68.

Freise, C., Erben, U., Muche, M., Farndale, R., Zeitz, M., Somasundaram, R., Ruehl, M., 2009. The alpha 2 chain of collagen type VI sequesters latent proforms of matrix-metalloproteinases and modulates their activation and activity. Matrix Biol 28, 480-489.

Frey, N., Olson, E.N., 2003. Cardiac hypertrophy: the good, the bad, and the ugly. Annual review of physiology 65, 45-79.

Ge, J., Zhao, G., Chen, R., Li, S., Wang, S., Zhang, X., Zhuang, Y., Du, J., Yu, X., Li, G., Yang, Y., 2006. Enhanced myocardial cathepsin B expression in patients with dilated cardiomyopathy. European journal of heart failure 8, 284-289.

Giusti, I., D'Ascenzo, S., Millimaggi, D., Taraboletti, G., Carta, G., Franceschini, N., Pavan, A., Dolo, V., 2008. Cathepsin B Mediates the pH-Dependent Proinvasive Activity of Tumor-Shed Microvesicles. Neoplasia (New York, N.Y.) 10, 481-488.

Greco, M.R., Antelmi, E., Busco, G., Guerra, L., Rubino, R., Casavola, V., Reshkin, S.J., Cardone, R.A., 2014. Protease activity at invadopodial focal digestive areas is dependent on NHE1-driven acidic pHe. Oncology reports 31, 940-946.

Heineke, J., Molkentin, J.D., 2006. Regulation of cardiac hypertrophy by intracellular signalling pathways. Nature reviews. Molecular cell biology 7, 589-600.

Hescheler, J., Meyer, R., Plant, S., Krautwurst, D., Rosenthal, W., Schultz, G., 1991. Morphological, biochemical, and electrophysiological characterization of a clonal cell (H9c2) line from rat heart. Circulation Research 69, 1476-1486.

Ishidoh, K., Kominami, E., 1995. Procathepsin L degrades extracellular matrix proteins in the presence of glycosaminoglycans in vitro. Biochemical and biophysical research communications 217, 624-631.

Javadov, S., Choi, A., Rajapurohitam, V., Zeidan, A., Basnakian, A.G., Karmazyn, M., 2008. NHE-1 inhibition-induced cardioprotection against ischaemia/reperfusion is associated with attenuation of the mitochondrial permeability transition. Cardiovascular research 77, 416-424.

Javadov, S., Rajapurohitam, V., Kilic, A., Zeidan, A., Choi, A., Karmazyn, M., 2009. Anti-hypertrophic effect of NHE-1 inhibition involves GSK-3beta-dependent attenuation of mitochondrial dysfunction. Journal of molecular and cellular cardiology 46, 998-1007.

Kang, P.M., Izumo, S., 2003. Apoptosis in heart: basic mechanisms and implications in cardiovascular diseases. Trends in Molecular Medicine 9, 177-182.

Kehat, I., Molkentin, J.D., 2010. Molecular pathways underlying cardiac remodeling during pathophysiological stimulation. Circulation 122, 2727-2735.

Kostoulas, G., Lang, A., Nagase, H., Baici, A., 1999. Stimulation of angiogenesis through cathepsin B inactivation of the tissue inhibitors of matrix metalloproteinases. FEBS letters 455, 286-290.

Levine, B., Kroemer, G., 2008. Autophagy in the pathogenesis of disease. Cell 132, 27-42.

Li, C., Li, F., Zhao, K., Yao, J., Cheng, Y., Zhao, L., Li, Z., Lu, N., Guo, Q., 2014. LFG-500 inhibits the invasion of cancer cells via down-regulation of PI3K/AKT/NF-kappaB signaling pathway. PloS one 9, e91332.

Liu, A., Gao, X., Zhang, Q., Cui, L., 2013. Cathepsin B inhibition attenuates cardiac dysfunction and remodeling following myocardial infarction by inhibiting the NLRP3 pathway. Molecular medicine reports 8, 361-366.

Malo, M.E., Fliegel, L., 2006. Physiological role and regulation of the Na+/H+ exchanger. Canadian journal of physiology and pharmacology 84, 1081-1095.

Marano, G., Vergari, A., Catalano, L., Gaudi, S., Palazzesi, S., Musumeci, M., Stati, T., Ferrari, A.U., 2004. Na+/H+ exchange inhibition attenuates left ventricular remodeling and preserves systolic function in pressure-overloaded hearts. British journal of pharmacology 141, 526-532.

Mathers CD, L.D., 2006. Projections of Global Mortality and Burden of Disease from 2002 to 2030. PLOS Medicine 3.

Merten, K.E., Jiang, Y., Feng, W., Kang, Y.J., 2006. Calcineurin activation is not necessary for Doxorubicin-induced hypertrophy in H9c2 embryonic rat cardiac cells: involvement of the phosphoinositide 3-kinase-Akt pathway. The Journal of pharmacology and experimental therapeutics 319, 934-940.

Mizushima, N., Yoshimori, T., 2007. How to Interpret LC3 Immunoblotting. Autophagy 3, 542-545.

Mlih, M., Abdulrahman, N., Gadeau, A.P., Mohamed, I.A., Jaballah, M., Mraiche, F., 2015. Na(+)/H (+) exchanger isoform 1 induced osteopontin expression in cardiomyocytes involves NFAT3/Gata4. Molecular and cellular biochemistry 404, 211-220.

Mohamed, I.A., Mraiche, F., 2015. Targeting osteopontin, the silent partner of Na+/H+ exchanger isoform 1 in cardiac remodeling. Journal of cellular physiology 230, 2006-2018.

Mraiche, F., Fliegel, L., 2011. Elevated expression of activated Na(+)/H(+) exchanger protein induces hypertrophy in isolated rat neonatal ventricular cardiomyocytes. Molecular and cellular biochemistry 358, 179-187.

Müller, A., Dhalla, N., 2012. Role of various proteases in cardiac remodeling and progression of heart failure. Heart Fail Rev 17, 395-409.

Mundel, P., Reiser, J., 2010. Proteinuria: an enzymatic disease of the podocyte? Kidney Int 77, 571-580.

Pan, L., Li, Y., Jia, L., Qin, Y., Qi, G., Cheng, J., Qi, Y., Li, H., Du, J., 2012. Cathepsin S deficiency results in abnormal accumulation of autophagosomes in macrophages and enhances Ang II-induced cardiac inflammation. PloS one 7, e35315.

Pungercar, J.R., Caglic, D., Sajid, M., Dolinar, M., Vasiljeva, O., Pozgan, U., Turk, D., Bogyo, M., Turk, V., Turk, B., 2009. Autocatalytic processing of procathepsin B is triggered by proenzyme activity. FEBS J 276, 660-668.

Riaz, S., 2016. Cathepsin B Induced Cardiomyocyte Hypertrophy Requires Activation of The Na+/H+ Exchanger Isoform-1, Master's Thesis, College of Pharmacy. Qatar University, Qatar.

Rodriguez, D., Morrison, C.J., Overall, C.M., 2010. Matrix metalloproteinases: what do they not do? New substrates and biological roles identified by murine models and proteomics. Biochimica et biophysica acta 1803, 39-54.

546 Rozhin, J., Sameni, M., Ziegler, G., Sloane, B.F., 1994. Pericellular pH affects distribution
547 and secretion of cathepsin B in malignant cells. Cancer Res 54, 6517-6525.
548 Sandri, M., 2013. Protein breakdown in muscle wasting: Role of autophagy-lysosome and
549 ubiquitin-proteasome()(). Int J Biochem Cell Biol 45, 2121-2129.
550 Singh, R., Dandekar, S., Elimban, V., Gupta, S., Dhalla, N., 2004. Role of proteases in the
551 pathophysiology of cardiac disease. Molecular and cellular biochemistry 263, 241-256.
552 Solli, A.I., Fadnes, B., Winberg, J.O., Uhlin-Hansen, L., Hadler-Olsen, E., 2013. Tissue- and
553 cell-specific co-localization of intracellular gelatinolytic activity and matrix
554 metalloproteinase 2. J Histochem Cytochem 61, 444-461.
555 Sotanaphun, U., Phattanawasin, P., Sriphong, L., 2009. Application of Scion image software
556 to the simultaneous determination of curcuminoids in turmeric (Curcuma longa).
557 Phytochemical analysis : PCA 20, 19-23.
558 Steffan, J.J., Snider, J.L., Skalli, O., Welbourne, T., Cardelli, J.A., 2009. Na+/H+ exchangers
559 and RhoA regulate acidic extracellular pH-induced lysosome trafficking in prostate cancer
560 cells. Traffic 10, 737-753.
561 Stempien-Otero, A., Plawman, A., Meznarich, J., Dyamenahalli, T., Otsuka, G., Dichek,
562 D.A., 2006. Mechanisms of cardiac fibrosis induced by urokinase plasminogen activator. The
563 Journal of biological chemistry 281, 15345-15351.
564 Sun, M., Chen, M., Liu, Y., Fukuoka, M., Zhou, K., Li, G., Dawood, F., Gramolini, A., Liu,
565 P.P., 2011. Cathepsin-L contributes to cardiac repair and remodelling post-infarction.
566 Cardiovascular research 89, 374-383.
567 Sun, M., Ouzounian, M., de Couto, G., Chen, M., Yan, R., Fukuoka, M., Li, G., Moon, M.,
568 Liu, Y., Gramolini, A., Wells, G.J., Liu, P.P., 2013. Cathepsin-L ameliorates cardiac
569 hypertrophy through activation of the autophagy-lysosomal dependent protein processing
570 pathways. Journal of the American Heart Association 2, e000191.

571 Tanida, I., Ueno, T., Kominami, E., 2008. LC3 and Autophagy. Methods Mol. Biol. 445, 77-
572 88.
573 Taves, J., Rastedt, D., Canine, J., Mork, D., Wallert, M.A., Provost, J.J., 2008. Sodium
574 hydrogen exchanger and phospholipase D are required for alpha1-adrenergic receptor
575 stimulation of metalloproteinase-9 and cellular invasion in CCL39 fibroblasts. Archives of
576 biochemistry and biophysics 477, 60-66.
577 Togashi, K., Wakatsuki, S., Furuno, A., Tokunaga, S., Nagai, Y., Araki, T., 2013. Na+/H+
578 exchangers induce autophagy in neurons and inhibit polyglutamine-induced aggregate
579 formation. PloS one 8, e81313.
580 Watkins, S.J., Borthwick, G.M., Arthur, H.M., 2011. The H9C2 cell line and primary
581 neonatal cardiomyocyte cells show similar hypertrophic responses in vitro. In vitro cellular &
582 developmental biology. Animal 47, 125-131.
583 Weng, C.H., Chung, F.P., Chen, Y.C., Lin, S.F., Huang, P.H., Kuo, T.B., Hsu, W.H., Su,
584 W.C., Sung, Y.L., Lin, Y.J., Chang, S.L., Lo, L.W., Yeh, H.I., Chen, Y.J., Hong, Y.R., Chen,
585 S.A., Hu, Y.F., 2016. Pleiotropic Effects of Myocardial MMP-9 Inhibition to Prevent
586 Ventricular Arrhythmia. Scientific reports 6, 38894.
587 WHO, 2011. Global status report on noncommunicable disaeses 2010.
588 WHO, 2013. Cardiovascular diseases key facts.
589 Wilson EM, S.F., 2001. Myocardial remodelling and matrix metalloproteinases in heart
590 failure: turmoil within the interstitium. Annals of Medicine 33, 623-634.
591 Wu, Q.Q., Xu, M., Yuan, Y., Li, F.F., Yang, Z., Liu, Y., Zhou, M.Q., Bian, Z.Y., Deng, W.,
592 Gao, L., Li, H., Tang, Q.Z., 2015. Cathepsin B deficiency attenuates cardiac remodeling in
593 response to pressure overload via TNFalpha/ASK1/JNK pathway. American journal of
594 physiology. Heart and circulatory physiology, ajpheart.00601.02014.

595 Xue, J., Mraiche, F., Zhou, D., Karmazyn, M., Oka, T., Fliegel, L., Haddad, G.G., 2010.
596 Elevated myocardial Na+/H+ exchanger isoform 1 activity elicits gene expression that leads
597 to cardiac hypertrophy. Physiological genomics 42, 374-383.
598 Zhao, J., Brault, J.J., Schild, A., Cao, P., Sandri, M., Schiaffino, S., Lecker, S.H., Goldberg,
599 A.L., 2007. FoxO3 coordinately activates protein degradation by the autophagic/lysosomal
600 and proteasomal pathways in atrophying muscle cells. Cell Metab 6, 472-483.
601

Fig 1. Effects of Angiotensin II on cathepsin B (Cat B) protein expression. (A) Representative Western blot of Cat B protein expression in cell lysates of H9c2 cardiomyoblasts treated with 1 μM, 10 μM, 100 μM, 1 nM, 10 nM or 100 nM Ang II for 24 h. Immunoblotting was against pro-Cat B (37 kDa) and active-CatB (25 kDa) and α-tubulin (50 kDa). (B) Bar graphs representing quantification of relative levels of Cat B protein expression (n=7) normalized to α-tubulin. Results are expressed as a % control (non-treated (NT)) ± %S.E.M. *P < 0.05 vs. control. Ang II, angiotensin II; Cat B, cathepsin B; NT, non-treated.

Fig 2. Influence of inhibition of NHE1 or cathepsin B (Cat B) on the hypertrophic phenotype of H9c2 cardiomyoblasts. (A) Representative DNA agarose gel of ANP and β-actin mRNA expression in H9c2 cardiomyoblasts treated with Ang II in the presence or absence of EMD or CA-074Me for 24 h. (B) Bar graphs representing quantification of ANP mRNA expression in H9c2 cardiomyoblasts normalized to β-actin (n=7). Results are expressed as a % of control (non-treated (NT)) ± %S.E.M. *P < 0.05 vs. control, #P < 0.05 vs. Ang II. (C) Protein content of H9c2 cardiomyoblasts treated with Ang II in the presence and absence of EMD or CA-074Me for 24 h expressed as % of control (n=4). (D) Representative crystal violet stained microscopy images of H9c2 cardiomyoblasts treated with Ang II in the presence and absence of EMD or CA-074Me for 24 h. (E) Cell surface area of at least 30-40 H9c2 cardiomyoblasts from 3-4 individual dishes (n=4). Results are expressed as a % of control (non-treated (NT)) ± %S.E.M. *P < 0.05 vs. control, #P < 0.05 vs. Ang II. Ang II, angiotensin II; ANP, atrial natriuretic peptide; DNA, deoxyribonucleic acid; NT, non-treated.

Fig 3. Influence of inhibition of NHE1 by EMD on cathepsin B (Cat B) protein and gene expression. (A) Representative Western blot of Cat B protein expression in cell lysates of

H9c2 cardiomyoblasts treated with Ang II in the presence or absence of EMD or CA- 074Me for 24 h. Immunoblotting was against pro-Cat B (37 kDa) and active-CatB (25 kDa) and α-tubulin (50 kDa). (B) Quantification of relative levels of Cat B protein expression (n=6-7) normalized to α-tubulin. Results are expressed as a % of control (non- treated (NT)) ± %S.E.M. *P < 0.05 vs. control, #P < 0.05 vs. Ang II. (C) Representative agarose DNA gel of cathepsin B mRNA expression in H9c2 cardiomyoblasts treated with Ang II in the presence or absence of EMD or CA-074Me for 24 h. cDNA amplification was against Cat B and β-actin. (D) Quantification of Cat B mRNA expression in H9c2 cardiomyoblasts normalized to β-actin (n=7). Results are expressed as % of control (non- treated (NT)) ± %S.E.M. *P < 0.05 vs. control, #P < 0.05 vs. Ang II. Ang II, angiotensin II; Cat B, cathepsin B; DNA, deoxyribonucleic acid; NT, non-treated.

Fig 4. Influence of inhibition of NHE1 or cathepsin B (Cat B) on lysosomal integrity. (A) Representative fluorescent images of the intracellular localization and morphology of lysosomes of H9c2 cardiomyoblasts treated with Ang II in the presence or absence of EMD or CA-074Me. H9c2 cardiomyoblasts were stained with the acidic probe, Lysotracker Red (n=3). **Influence of inhibition of NHE1 or cathepsin B on MMP-9 in the extracellular environment.** (B) Representative Western blot of Cat B protein expression in the media of H9c2 cardiomyoblasts treated with Ang II in the presence or absence of EMD or CA-074Me for 24 h. Immunoblotting was against pro-Cat B (37 kDa). (C) Quantification of the relative levels of Cat B protein expression (n=5). Results are expressed as a % of control (non-treated (NT)) ± % S.E.M. *P < 0.05 vs. control, #P < 0.05 vs. Ang II. (D) Inhibition of NHE1 or Cat B reduces MMP-9 gelatinolytic activity. Representative zymogram of MMP-9 gelatinolytic activity in conditioned media from H9c2 cardiomyoblasts treated with Ang II in the presence or absence of EMD or CA-074Me for 24 h. (E) Quantification of MMP-9 gelatinolytic activity in H9c2 cardiomyoblasts (n=3). Results are expressed as a % of control (non-treated

(NT)) ± %S.E.M. *P < 0.05 vs. control, #P < 0.05 vs. Ang II. Ang II, angiotensin II; Cat B, cathepsin B; MMP-9, matrix metalloproteinase-9.

Fig 5. Influence of inhibition of NHE1 or cathepsin B (Cat B) on autophagy. (A) Representative Western blot of LC3 protein expression of H9c2 cardiomyoblasts treated with Ang II in the presence and absence of EMD or CA-074Me for 24 hours. Immunoblotting was against LC3-I and II (14 and 16 kDa). (B) Quantification of relative levels of LC3-II to LC3-I protein expression (n=5). Results are expressed as a % of control (non-treated (NT)) ± %S.E.M. *P < 0.05 vs. control, #P < 0.05 vs. Ang II. Ang II, angiotensin II; NT, non-treated.

Fig 6. Schematic Diagram Illustrating Pathway by Which Inhibition of NHE1-reduces cathepsin B induced cardiomyocyte-hypertrophy through the inhibition of MMP-9. The inhibition of NHE1 reduces cathepsin B protein and gene expression and MMP-9 activity, and cardiomyocyte hypertrophy. NHE1, Na^+/H^+ Exchanger 1; Cat B, cathepsin B; MMP-9, matrix metalloproteinase-9. Ang II, angiotensin II.

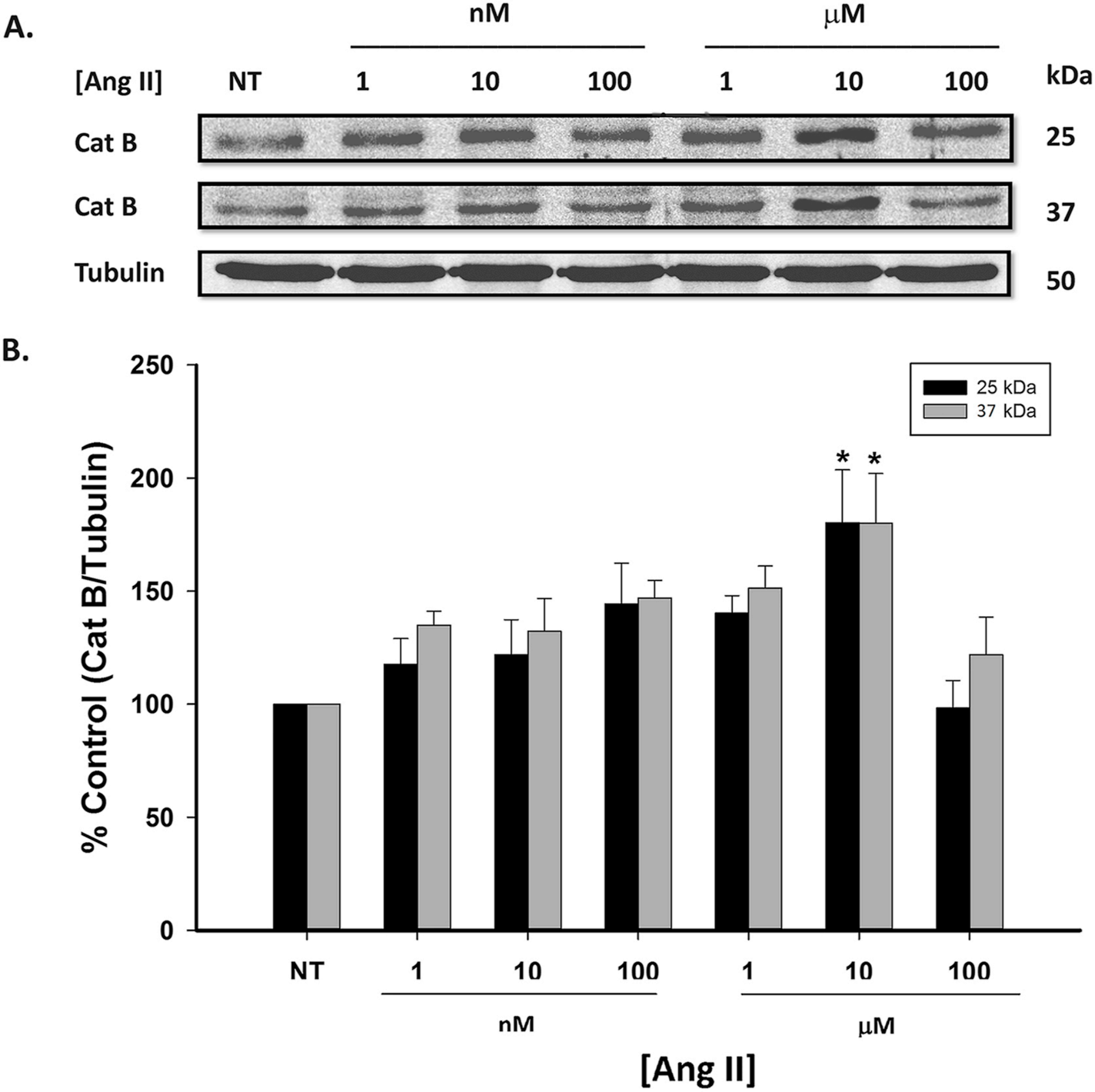
A.
nM
μM
[Ang II]
NT
1
10
100
1
10
100
kDa
Cat B
25
Cat B
37
Tubulin
50
B.
250
200
150
100
50
0
% Control (Cat B/Tubulin)
25 kDa
37 kDa
*
*
NT
1
10
100
1
10
100
nM
μM
[Ang II]

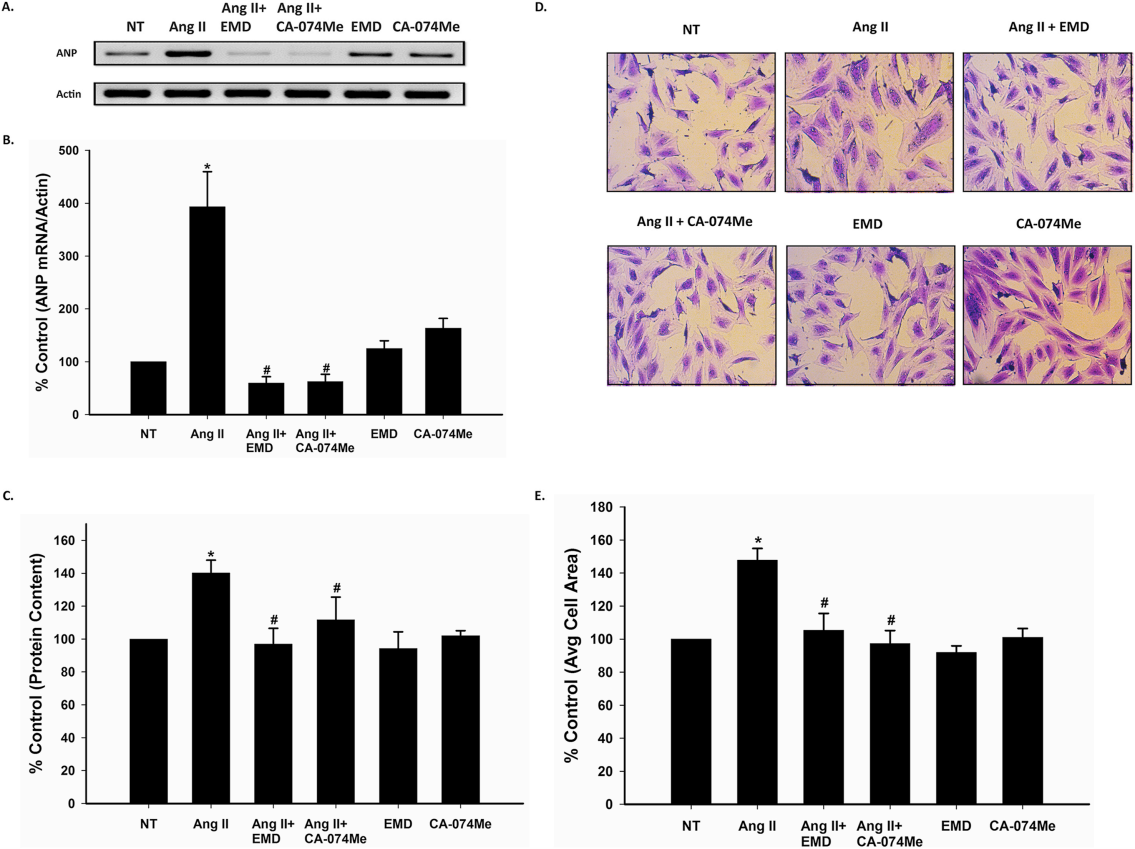
A.
NT
Ang II
Ang II+ EMD
Ang II+ CA-074Me
EMD
CA-074Me
ANP
Actin
B.
% Control (ANP mRNA/Actin)
500
400
300
200
100
0
*
#
#
NT
Ang II
Ang II+ EMD
Ang II+ CA-074Me
EMD
CA-074Me
D.
NT
Ang II
Ang II + EMD
Ang II + CA-074Me
EMD
CA-074Me
C.
% Control (Protein Content)
160
140
120
100
80
60
40
20
0
*
#
#
NT
Ang II
Ang II+ EMD
Ang II+ CA-074Me
EMD
CA-074Me
E.
% Control (Avg Cell Area)
180
160
140
120
100
80
60
40
20
0
*
#
#
NT
Ang II
Ang II+ EMD
Ang II+ CA-074Me
EMD
CA-074Me

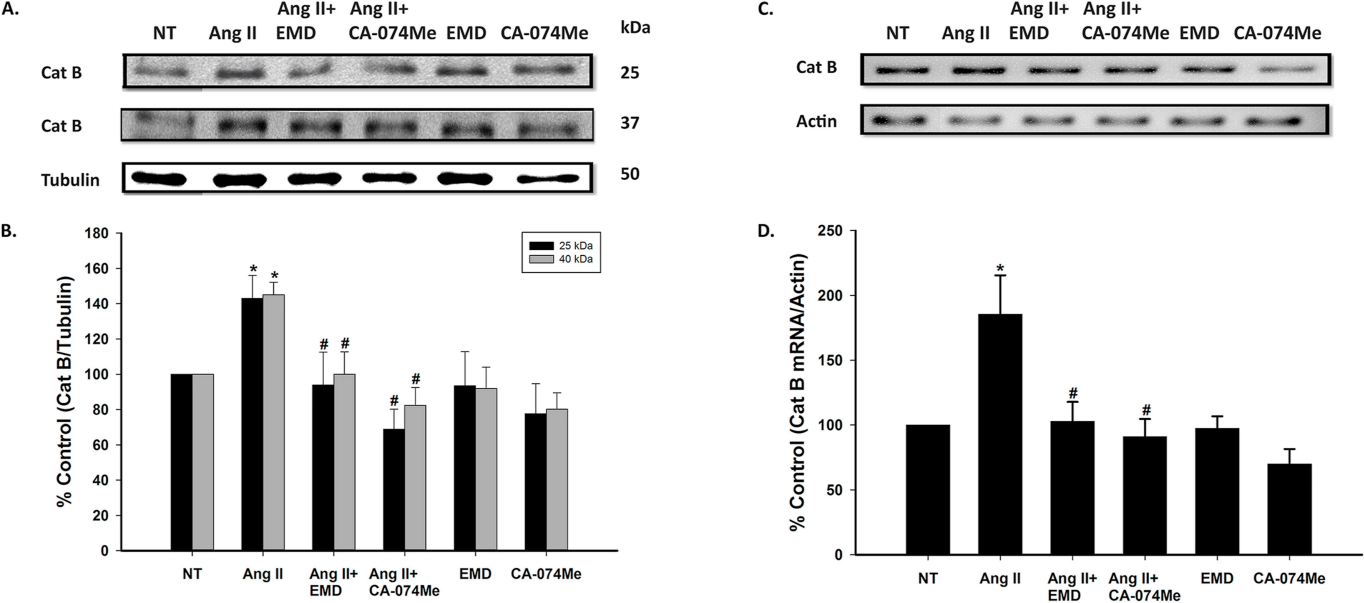
A.
NT
Ang II
Ang II+ EMD
Ang II+ CA-074Me
EMD
CA-074Me
kDa
Cat B
25
Cat B
37
Tubulin
50
C.
NT
Ang II
Ang II+ EMD
Ang II+ CA-074Me
EMD
CA-074Me
Cat B
Actin
B.
25 kDa
40 kDa
% Control (Cat B/Tubulin)
180
160
140
120
100
80
60
40
20
0
NT
Ang II
Ang II+ EMD
Ang II+ CA-074Me
EMD
CA-074Me
D.
% Control (Cat B mRNA/Actin)
250
200
150
100
50
0
NT
Ang II
Ang II+ EMD
Ang II+ CA-074Me
EMD
CA-074Me

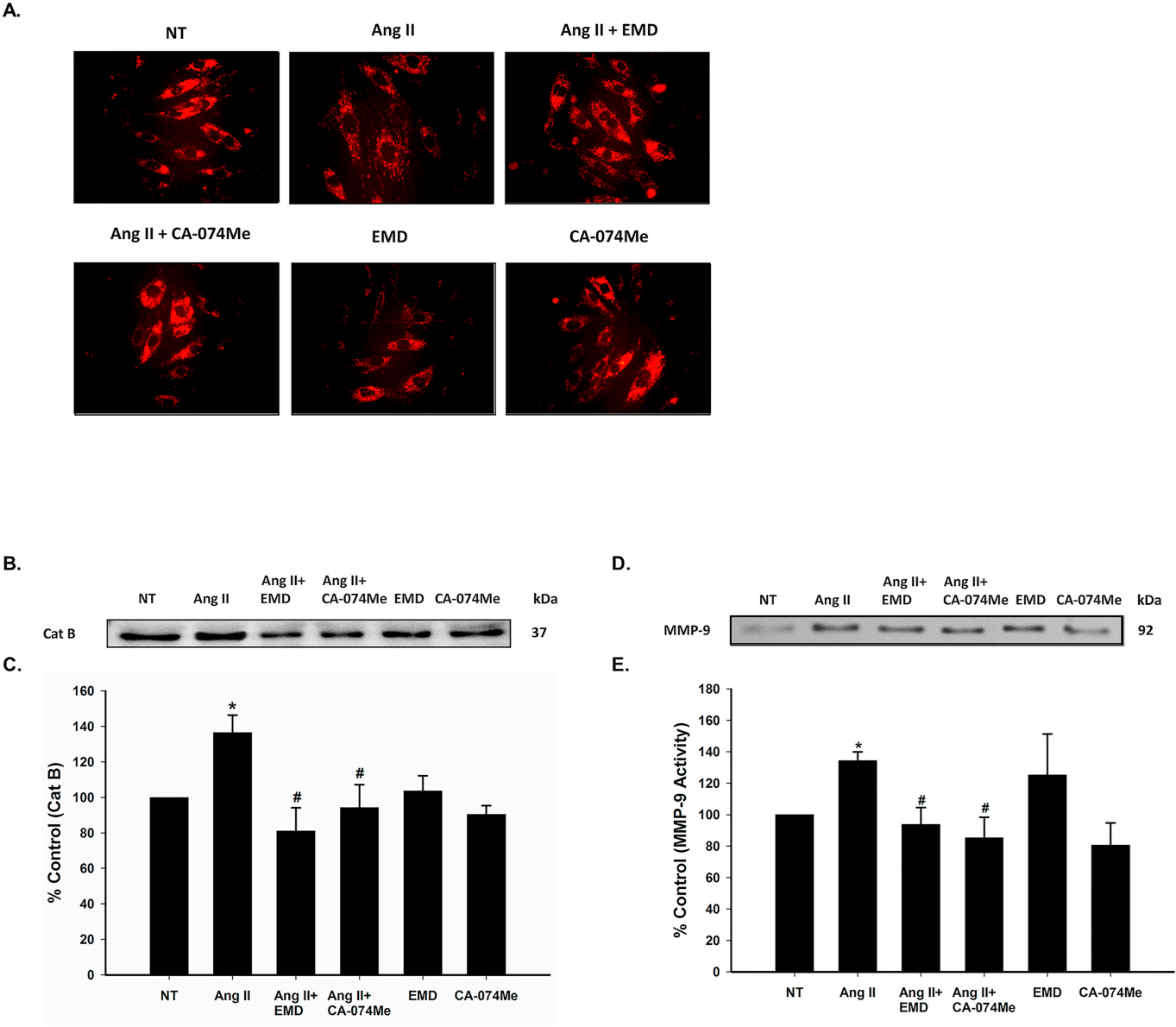
A.
NT
Ang II
Ang II + EMD
Ang II + CA-074Me
EMD
CA-074Me
B.
NT
Ang II
Ang II+ EMD
Ang II+ CA-074Me
EMD
CA-074Me
kDa
Cat B
37
C.
% Control (Cat B)
160
140
120
100
80
60
40
20
0
*
#
#
NT
Ang II
Ang II+ EMD
Ang II+ CA-074Me
EMD
CA-074Me
D.
NT
Ang II
Ang II+ EMD
Ang II+ CA-074Me
EMD
CA-074Me
kDa
MMP-9
92
E.
% Control (MMP-9 Activity)
180
160
140
120
100
80
60
40
20
0
*
#
#
NT
Ang II
Ang II+ EMD
Ang II+ CA-074Me
EMD
CA-074Me

A.

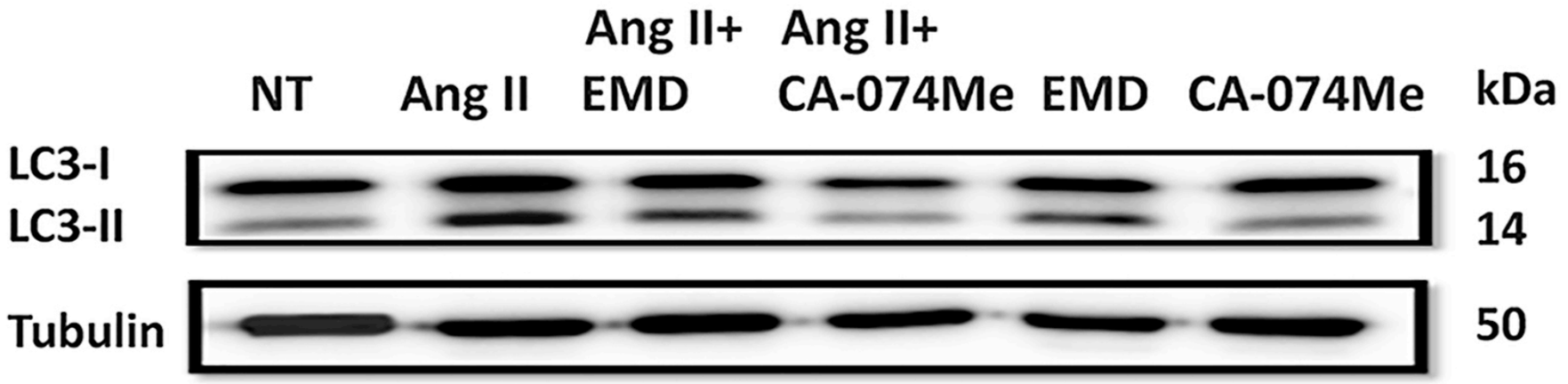
NT
Ang II
Ang II+ EMD
Ang II+ CA-074Me
EMD
CA-074Me
kDa
LC3-I
LC3-II
16
14
Tubulin
50

B.

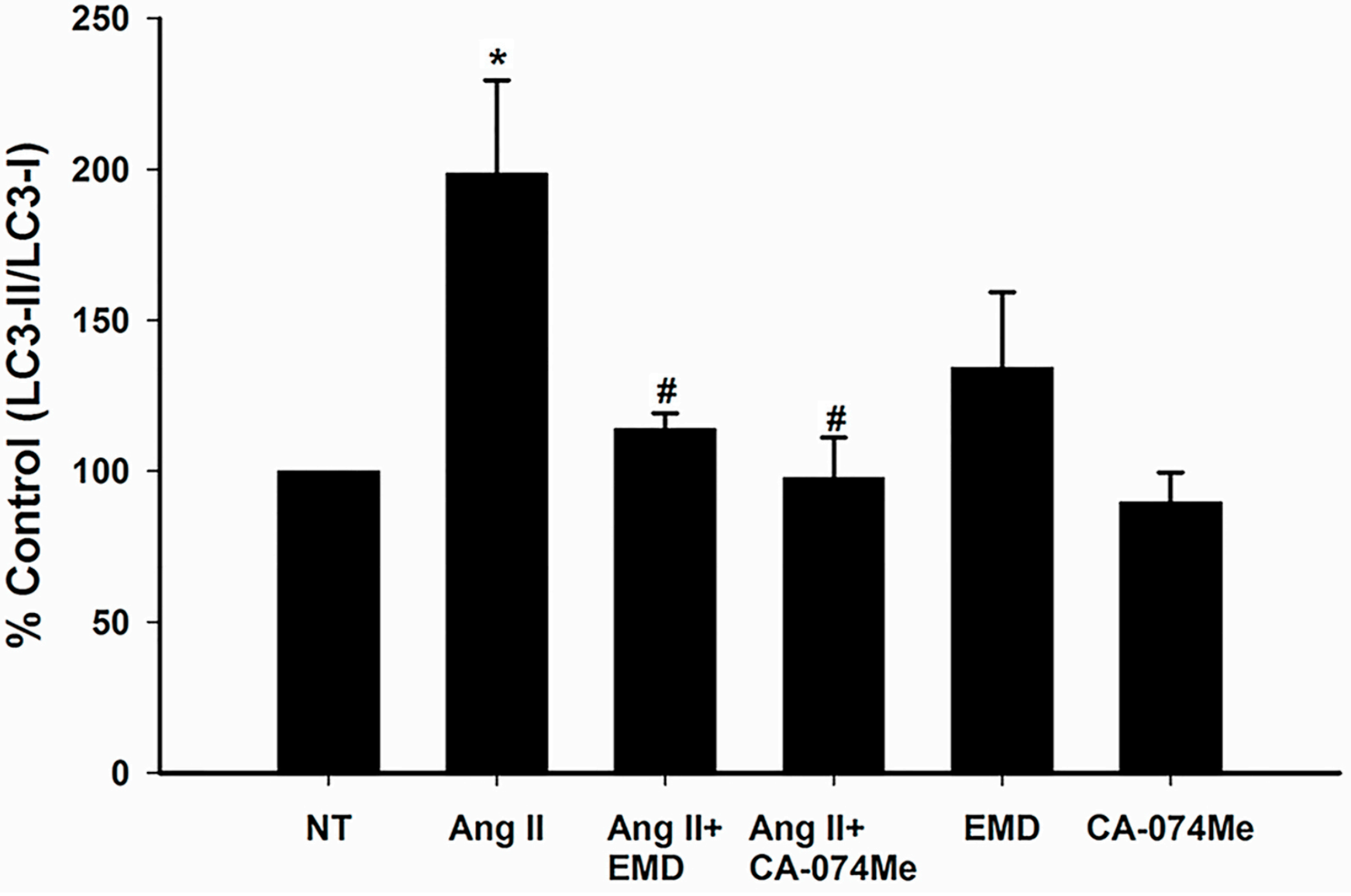
% Control (LC3-II/LC3-I)
250
200
150
100
50
0
*
#
#
NT
Ang II
Ang II+ EMD
Ang II+ CA-074Me
EMD
CA-074Me

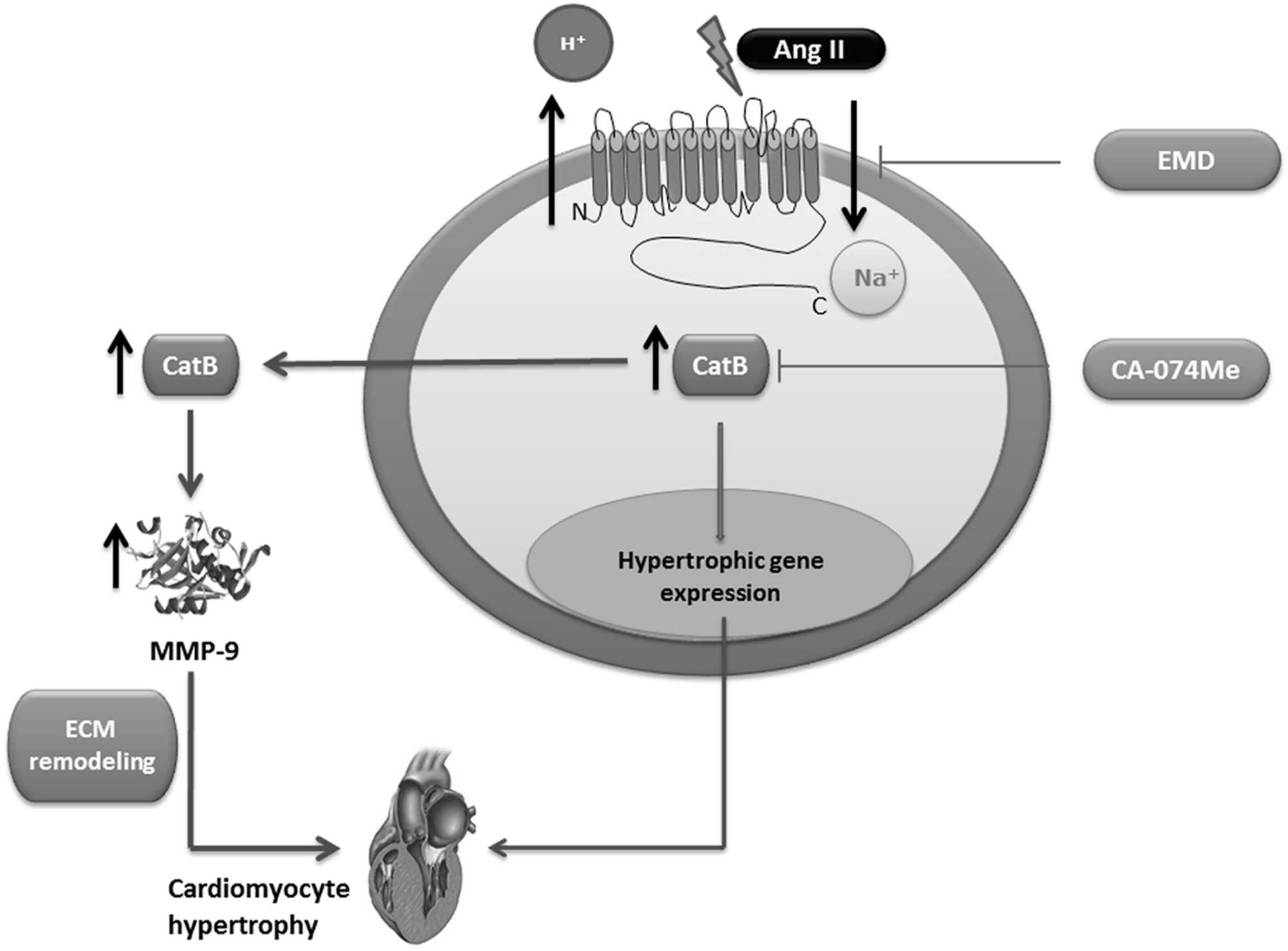
H+
Ang II
EMD
N
C
Na+
CatB
CatB
CA-074Me
MMP-9
Hypertrophic gene expression
ECM remodeling
Cardiomyocyte hypertrophy